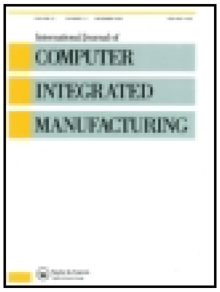

International Journal of Computer Integrated Manufacturing
Publication details, including instructions for authors and subscription information:
http://www.tandfonline.com/loi/tcim20

Assembly time modelling through connective complexity metrics

James L. Mathieson [a] , Bradley A. Wallace [a] & Joshua D. Summers [a]
[a] Department of Mechanical Engineering, Clemson Engineering Design Applications and Research (CEDAR), Clemson University, Clemson, SC, USA
Published online: 21 May 2012.

International Journal of Computer Integrated Manufacturing
2012, 1–13, i*First article*

Assembly time modelling through connective complexity metrics

James L. Mathieson, Bradley A. Wallace and Joshua D. Summers*

Department of Mechanical Engineering, Clemson Engineering Design Applications and Research (CEDAR), Clemson University, Clemson, SC, USA

(*Received 30 March 2011; final version received 18 March 2012*)

This paper presents an approach for the development of surrogate models predicting the assembly time of a system based on complexity metrics of the physical system architecture when detailed geometric information is unavailable. A convention for modelling physical architecture is presented, followed by a sample of 10 analysed systems used for training and three systems used for validation. These systems are evaluated on complexity metrics developed from graph theoretic measures. An example model is developed based on a series of regressions of trends observed within the sample data. This is validated against the systems that are not used to develop the model. The model developed uses average path length, part count and path length density to approximate assembly time within the standard deviation of the subjective variation possible in Boothroyd and Dewhurst design for assembly (DFA) analysis. While the specific example model developed is generalisable only to systems similar to those in the sample set, the capability to develop mappings between physical architecture and assembly time in early-stage design is demonstrated.

Keywords: design for assembly; complexity; modelling

1. Complexity in assembly

Complexity in design is often addressed indirectly through various analysis techniques which have been specially developed for a single purpose. Examples of this include design for X (DFX) analysis, where a procedure has been developed for evaluating a particular aspect of the design's performance. One such procedure is design for assembly (DFA) analysis. The purpose for DFA is to guide the design solution for a particular product in a manner which will ease the assembly process for the product. This is done through design rules and analysis methods which allow designs to be compared.

In the 1960s, many companies developed handbooks which guided designers in creating parts with manufacturing considerations (Boothroyd and Alting 1992). The emphasis of these design manuals was to produce and assemble many simple parts, which was thought at the time to be the cheapest method of manufacturing. However, this was before experimental and theoretical analyses were performed on the effects that part features had on the assembly time of the parts (Boothroyd 2005).

From such studies, Boothroyd and Dewhurst (Boothroyd and Dewhurst 1980, 1988, Boothroyd and Walker 1996) developed a DFA methodology which accurately quantifies and rates the producibility of designs for comparison (Priest and Sanchez 2001). The Boothroyd and Dewhurst DFA method aimed at minimising assembly times and costs by minimising the number of individual parts (Boothroyd and Dewhurst 1988), as well as optimising individual part design for ease of handling and joining (Warnecke and Babler 1988).

Other DFA methods include the Hitachi assembly evaluation method (AEM), the Lucas method (Leaney 1996) as well as Sony's design for cost effectiveness (DAC) (Yamigiwa *et al*. 1999). The Hitachi AEM decomposes each operation of an assembly into its basic operations. Each operation is then assigned a penalty score which is proportional to the operation's average time compared to the basic operation, a downward attachment. The score is then calculated by determining the average score of each of the individual parts and the total number of parts. The assembly time and cost for the product are then estimated from the product's AEM score (Ohashi *et al*. 2002).

The Lucas method uses functional, handling and fitting analyses (Mascle 2003). The functional analysis applies a design rule that the ratio of A/B, where A is the number of parts demanded by the design specifications, while B is the number of parts required by the particular design, is greater than 60% through the elimination of *B* parts (Boothroyd and Alting 1992,

*Corresponding author. Emails: Joshua.Summers@ces.clemson.edu; jsummer@clemson.edu

ISSN 0951-192X print/ISSN 1362-3052 online

http://dx.doi.org/10.1080/0951192X.2012.684706
http://www.tandfonline.com

Mital *et al.* 2008). The handling analysis introduces penalties based on each part's size, weight and handling difficulties. The fitting analysis adds penalties due to difficulties in the joining the individual parts (Boothroyd 1994, Leaney 1996, Mital *et al.* 2008).

In the Sony DAC methodology, each operation of assembly is given a unitless score out of 100 points. Simple operations have a lower score and higher operations have a higher score (Yamigiwa *et al.* 1999).

Since the development of formalised DFA methods, companies that have utilised them, such as Texas Instruments, Ford Motor Company, General Motors and Motorola (Boothroyd 2005) have achieved significant cost savings by producing fewer parts. The resulting parts are more complex but result in simpler product architecture (Boothroyd and Dewhurst 1988, Welter 1989).

However, all of the DFA methods discussed thus far require the designer to answer questions related to each individual part in an assembly. Many of the questions have subjective, rather than objective, answers. Other than the fact that the process can be extremely time consuming, the results will differ from one execution to another (Boothroyd and Alting 1992). As such, many DFA analyses tend to be used towards the end of the design process and not used iteratively through the design cycle (Dalgleish *et al.* 2000).

This paper seeks to counter the trend of applying DFA analysis only in late-stage design by exploring the possibility that complexity metrics may be used to develop surrogate models for assembly time approximation based on the physical architecture of the system without the need for exhaustive information from the designer. It is important to note that the purpose of this approach is not to supersede existing assembly time estimation methods currently applied in late-stage design or to achieve the same precision of those methods, but rather to enable the objective comparison of systems in early design prior to the availability of feature-level information. This will allow designers to consider the impacts of their decisions on assembly time earlier in the design process – when iteration is less costly – using concrete numbers rather than anecdotal experience. The first step to this goal is to establish the basis for modelling the connections in the physical system architecture.

2. Connectivity modelling

The modelling of system complexity for assembly requires that a representation of the system's architecture be developed. This is done by tracking the connections between the system's constituent elements in a bi-partite graph such as those shown in Figure 1 through Figure 3.

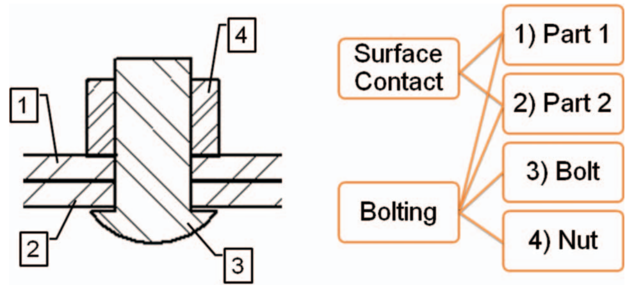

Figure 1. Bolting diagram.

In these graphs, connections are drawn between two independent sets. The first independent set is system elements or physical parts. This includes both major system components to be assembled as well as fastener components. These are drawn on the left side of the bi-partite graph.

The right side of the graph and the second independent set consists of relationships. As we are interested in system architecture, relationships tracked here are instances of connection and contact. For example, two parts may contact each other in one relationship, but also be fastened together using a nut and bolt in a different relationship. It is important to note that information on the size, location and specific geometry of each part and connection relationship is considered to be unavailable.

2.1. *Surface contact*

Contact between parts can involve multiple instances due to the geometry of parts. For example, two parts may contact each other through a flat surface on each part, a series of posts or interfacing contours. However, these contact conditions do not need to be fully defined in the connective model. Rather, it is sufficient to acknowledge that two parts contact each other outside of any given fastening instances. As such, there should be no more than one contact relationship between any two primary parts. Additionally, surface contact relationships should only be noted if this contact occurs outside of any fastening region. Future extensions may be explored with feature contacts, but they are currently deemed out of scope for this paper.

2.2. *Fasteners*

Fasteners are a type of relationship which can have a significant impact on the assembly time of the system. This is due to the introduction of additional system elements in the form of nuts, bolts, rivets and screws as well as the interaction of these fastening elements with the parts they are joining. To illustrate this, take the bolting diagram in Figure 1.

Here, we have two fastening elements, a nut (4) and a bolt (3), clamping together two parts (1 and 2). As this clamping interaction applies load through all of the elements and would not function in the absence of any given element, both of the parts as well as the nut and bolt are considered to be connected to a single relationship for the bolting as shown in Figure 2.

It should be noted that a unique system element is required for each physical element used. For example, a given item may be assembled using several identical screws. Rather than modelling these screws as a single element, each screw must exist as an independent element as it is in the physical system.

2.3. *Snap, press and interference fits*

Snap, press and interference fits are similar to fasteners in that they are a unique connection between parts separate from that of traditional surface contact. These features are more determinant than simple surface contacts and can impart the same general constraints as fasteners. However, the major difference in snapped connections is that there are no additional minor parts used in forming the connection while still being a unique relationship. This unique relationship captures the fact that each snap must still be aligned and engaged in assembly. Therefore, the connective relationship for a single snap fit would be arranged as in Figure 3. While additional snap fit instances would be modelled in the same manner, the lengths and tolerances of various instances are not differentiated.

2.4. *Other connections*

There are other forms of connections which require specific rules regarding how they are to be modelled in the graph. These include shafts, springs and electrical connections, each of which raise unique questions regarding the proper arrangement of elements and relationships. The guideline applied here is that these elements are, in effect, fasteners of one form or another.

This implies that, while each of these is a physical element, they are also related through a single relationship instance. As such, a shaft would be modelled as a shaft element connected to all of the elements attached along its length through a single shaft relationship. Similarly, a spring will be connected to the elements contacting it through a spring relationship.

Electrical connections pose a larger challenge as the form of connection to be made in assembly must be considered. If the connection is of a pre-made cord and plug, this may be modelled as a press or snap fit instance as that is exactly what this relationship is. However, if bare wires are to be joined, fastening elements such as crimps, twists and solder must be modelled individually as fasteners.

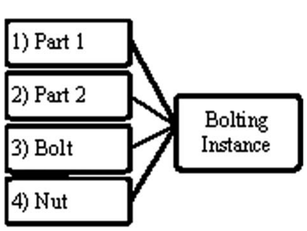

Figure 2. Bi-partite connectivity graph for bolting instance.

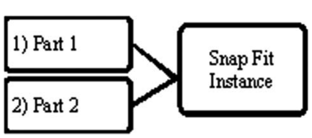

Figure 3. Bi-partite connectivity graph for snap-fit.

3. Complexity metrics

With sample systems established, a complexity analysis can be performed. This analysis addresses nine different metrics in three different classes. These classes are size metrics, path length metrics and decomposition metrics developed and presented in detail in Mathieson and Summers (2009, 2010). A review of these metrics is provided here for reference.

3.1. *Size*

Size metrics are the most common in complexity analysis (Ameri *et al.* 2008, Mathieson *et al.* 2009, Mathieson and Summers 2010, Summers and Shah 2010). These metrics address some count of entities within the system. Here, we address both dimensional and connective size properties.

Dimensional size addresses physical counts, particularly the elements and relationships in the system. The elements addressed in these systems are parts, including primary parts as well as any fastening parts. Relationships here are the connection instances which have been addressed in Section 2.

Connective size addresses the number of connections which have been made in the system. In simplest terms, connective size represents the number of lines which are drawn between elements and relationships in the bi-partite graph. Each of these connections represents an interface which must be established in assembly. However, also of interest is the number of properties which are available for change in the system. This is otherwise known as the system's parametric degree of freedom. This metric tracks the number of times each element is connected directly to another element.

3.2. Path length

Path length metrics are derived from an algorithmic treatment of the connective layout of the system. The result of this algorithm is a matrix of the number of connections which must be traversed in order to go from any given element to any other given element. This can then be used in conjunction with the established size metrics to produce general properties of the system's path lengths.

The first metric is total path length. This is the sum of the path length matrix and represents the number of connections traversed if every possible flow of system information were to be considered. Derived from this is the average path length. This is determined by dividing the total path length by the size of the path length matrix minus the empty identity. This will represent the average number of connections which must be traversed to go from any point in the system to any other point.

Additional metrics include path length density and maximum path length. The latter of these, maximum path length, is self-explanatory as it is simply the greatest number of connections which must be traversed to go between any two elements. Path length density is derived from average path length by again dividing this number by the number of relationships in the system, providing the average path length generated by any given relationship.

3.3. Decomposition

The final metric applied addresses the decomposability of the system. This is measured by the Ameri–Summers decomposability algorithm (Ameri *et al*. 2008). This is done by systematically breaking the least-connected relationships as so to isolate elements. The algorithm develops a score for the system based on how many steps are required to isolate the elements, how many elements can be isolated in each step, and the number of relationships which must be broken to isolate the elements in each step.

4. Training set

In order to identify a model which will approximate the results of DFA analysis, several systems with previously established assembly time estimates are needed. Five systems, automotive shifter, cylindrical Tweel™, electric knife, electric hand mixer and electric chopper, and their redesigns based on Boothroyd and Dewhurst DFA principles are introduced here. Four of these systems were analysed and redesigned as part of an undergraduate/graduate design for manufacturing course. One of the systems and redesign, the automotive shifter, is from an industry sponsored research and development project. The authors were only directly involved in the assembly time estimation of two of these systems, the Tweel™ and the electric knife. It is important to note that each assembly time analysis was done by a different individual. The analyses were taken as correct and not re-evaluated by the authors for this paper. These systems are then subjected to complexity analysis for use in the development of a predictive model.

4.1. Automotive shifter

The first system addressed is an automotive shifter unit. This is a relatively small item with only five primary parts and is used to represent a lower order of assembled systems.

4.1.1. Original

The original design of the shifter is heavily dependent on screw fasteners and multiple stages of assembly. Some parts are joined by as many as five screws. Only the connection between Parts 4 and 5 is done through a snap-fit clip. Figure 4 illustrates the assembly of the shifter in detail. In Boothroyd and Dewhurst assembly time analysis, the shifter was estimated to require 104.56 s to assemble. However, it should be noted that in practice the manufacturer observed an average assembly time of 105.24 s, highlighting the approximate nature of traditional DFA analysis.

4.1.2. Redesign

The shifter was redesigned based on established DFA principles with an eye towards lazy parts. A lazy part is one that does not serve any unique functional purpose in the final assembly. In the shifter, Part 2 is a trim cover which attaches onto another piece of trim. As this cover and trim combination does not perform separate function in the final assembly, these parts can be combined to a single part. This frees up the switch to attach directly to the central mount with a clip. These changes are reflected by the assembly diagram in Figure 5. The assembly time for this design by Boothroyd and Dewhurst assembly time estimation is 42.60 s.

4.2. Cylinder Tweel™

The second system is a meta-material Tweel™ prototype. This system utilises 225 metallic cylinders attached to inner and outer hoops to mimic the shear properties of polyurethane in a standard Tweel™. As a result, this system contains a very high number of parts and connections and thus represents an upper order of assembled systems.

4.2.1. Original

The original cylinder Tweel™ prototype makes heavy use of bolted connections. For each of the 225 cylinders, there is a bolted connection on both top and bottom. In addition to this, the 15 spoke-hub bars are attached by three bolted connections each. This makes for 495 bolted connections and twice that number in fastening parts. An illustration of this design is shown in Figure 6. The

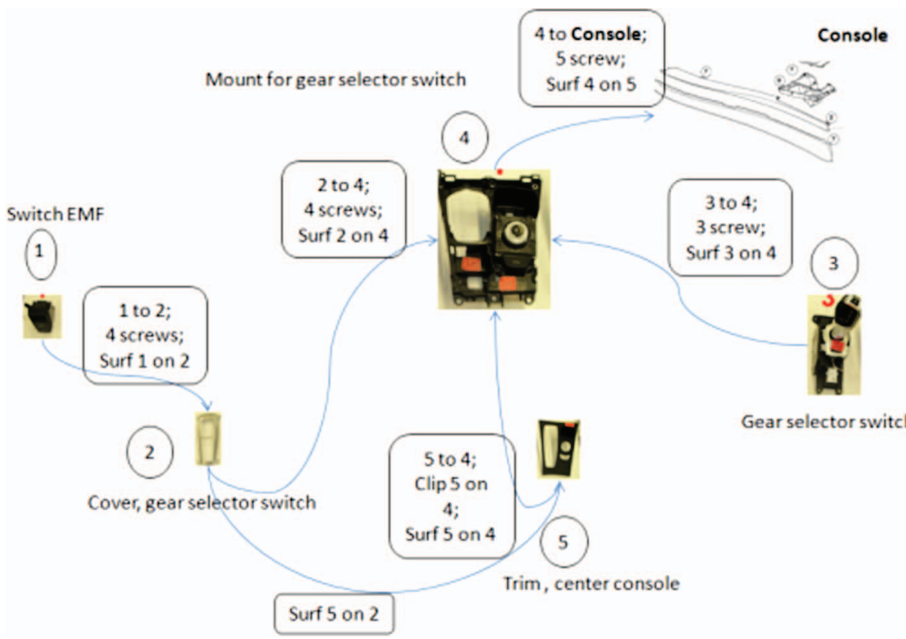

Figure 4. Original shifter.

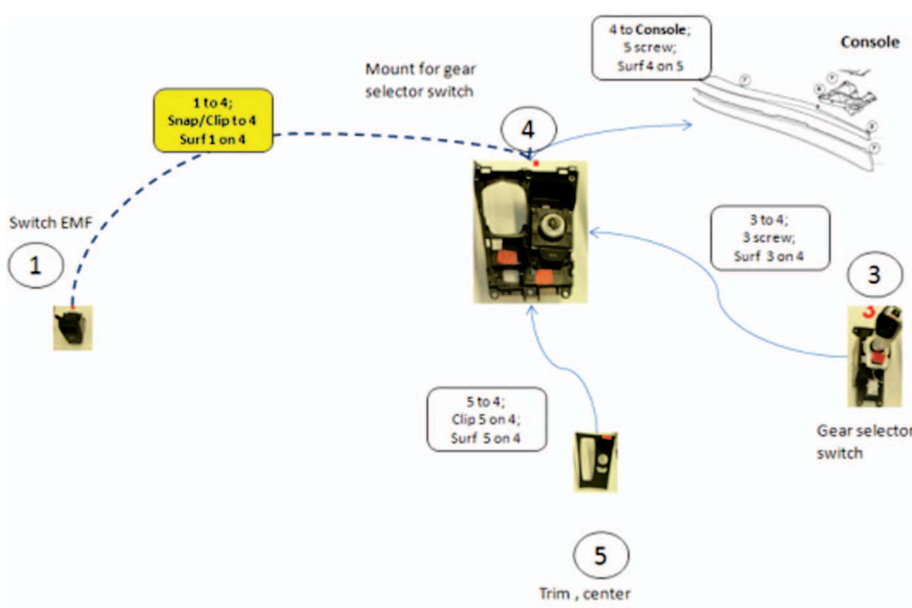

Figure 5. Redesigned shifter.

assembly time for this design is estimated by Boothroyd and Dewhurst assembly time analysis to be 13, 561.34 s or just over 3 h and 45 min.

4.2.2. Redesign

The redesign of the cylinder Tweel™ prototype focuses on reducing the number of fasteners and particularly on eliminated bolted connections. As a result, the shear cylinders are held in place by snap-fit fasteners which affix one row of cylinders at a time, rather than individually as with bolted connections. The spoke-hub bars are held in place by rings integrated into the hub and a cap plate on either side of the hub. These plates are affixed to the hub by three bolted connections. This is illustrated in Figure 7. The assembly time is estimated by Boothroyd and Dewhurst assembly time analysis to be 4925 s or 1 h and 22 min.

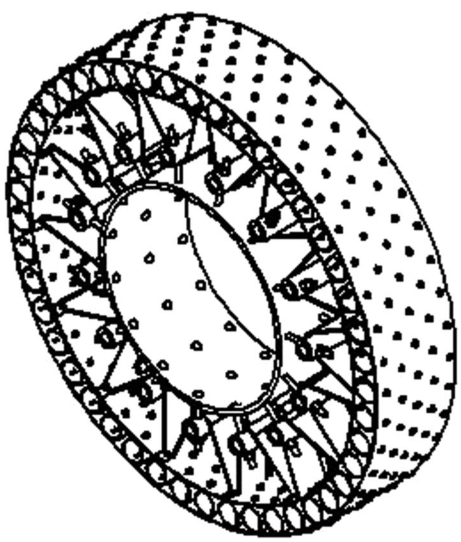

Figure 6. Original cylinder Tweel™.

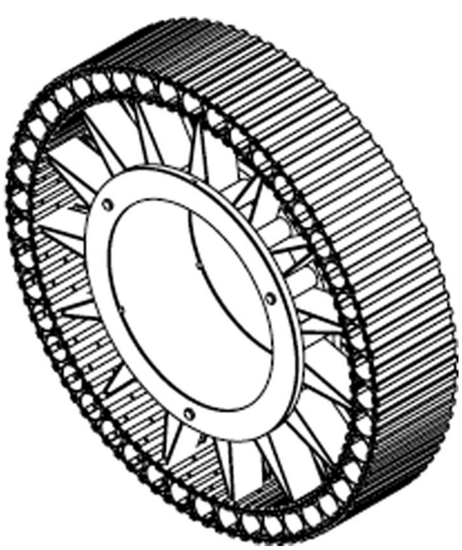

Figure 7. Redesigned cylinder Tweel™.

4.3. Electric knife

The third system is a consumer electric knife typically used for carving large meats and slicing uncut loaves of bread. This cutting action is achieved by a pair of adjacent reciprocating blades. These blades also can be ejected from the unit for washing. This ejection functionality and the linear motion of the reciprocating blades make this system relatively more complex than similar consumer appliances.

4.3.1. Original

The original electric knife design contains a large number of fasteners for its size. The majority of these fasteners are screws used to affix the major internal components to the base of the unit. However, most notable is the large number of springs used. There is one spring for each exterior button as well as two springs on each blade mount for a tensioning plunger and the blade clip. Figure 8 shows the numerous screw holes in the base as well as the two spring fasteners on the blade mounting arm. The assembly time for this design by Boothroyd and Dewhurst assembly time estimation is 325 s.

4.3.2. Redesign

The redesign of the electric knife addresses the issue of fasteners. Particularly, this is done by eliminating fastenings which are unnecessary to fully restrain the joined parts as well as fastening as many primary parts as possible with each fastener. Additionally, the spring used to tension the blades in each blade mount is

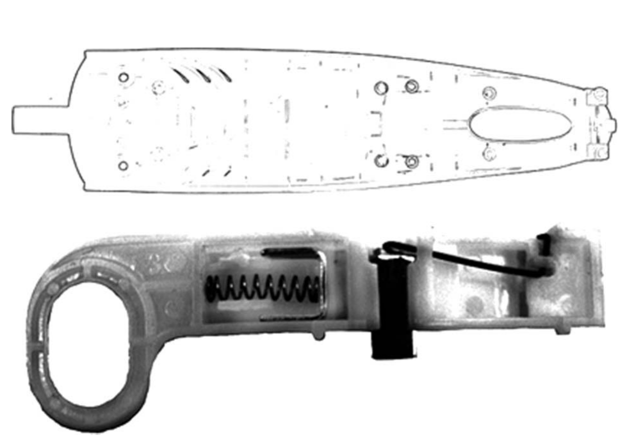

Figure 8. Original electric knife housing and blade mount.

replaced with a compliant mechanism integrated into the polymer blade mount. These alterations can be seen in Figure 9. The assembly time for this design by Boothroyd and Dewhurst assembly time estimation is 240 s.

4.4. Electric hand mixer

The fourth system is a consumer electric hand mixer. This system is composed of 15 primary parts. These parts are joining using snap fits, slide fits and traditional hardware fasteners.

4.4.1. Original

The original mixer design, shown in Figure 10, is composed of three cover sections attached with a total of six screws. The motor was mounted in the casing with four screws. The power cord was connected to the mixers wiring system via a clamp and two screws. The rest of the parts are assembled

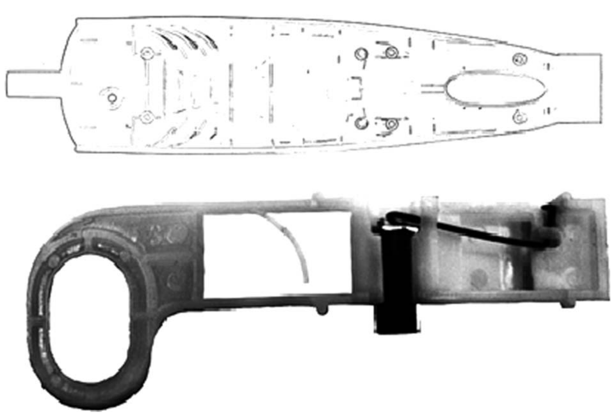

Figure 9. Redesigned electric knife housing and blade mount.

via slide fits. Three parts, the beaters and the speed control, are also spring loaded, which increases their assembly times. The assembly time for this design by Boothroyd and Dewhurst assembly time estimation is 130.45 s.

4.4.2. Redesign

The hand mixer was redesigned with an emphasis on eliminating unnecessary fasteners, which would eliminate the total number of parts in the assembly. All but one of the screws previously used to attach the cover pieces were removed and replaced with snap fits. The number of screws used to attach the motor to the inside of the cover pieces was reduced from four to two. The screws used to hold the power cord were replaced as they were deemed unnecessary to hold the cord within the mixers enclosure. The assembly time for this design by Boothroyd and Dewhurst assembly time estimation is 74.7 s.

4.5. Electric chopper

The fifth and final system is a small consumer electric blender, representing another product on the same scale as the hand mixer. The blender was made of mostly injection moulded parts connected using fasteners and snap fits.

4.5.1. Original

The original design, shown in Figure 11, contained three main subsystems: the container, the housing and the drive system. The housing system contained the majority of the fasteners in the system, with a total of 11 screws. The drive system also contained two screws. The container subsystem was attached to the housing using a twisting motion. The rest of the assembly

Figure 10. Original electric hand mixer.

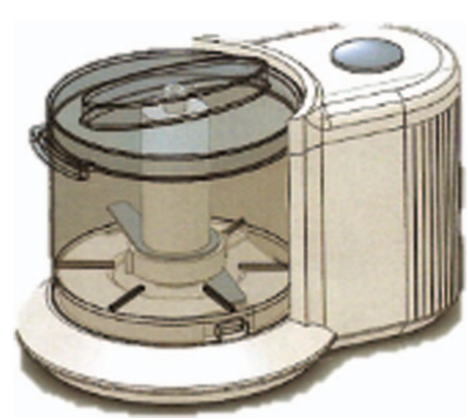

Figure 11. Original electric chopper.

process consisted of snap and slide fits. The assembly time for this design by Boothroyd and Dewhurst assembly time estimation is 228.5 s.

4.5.2. Redesign

A redesign was completed by determining which parts had the lowest design process efficiencies. The container subsystem was redesigned so that the twisting operation was no longer necessary. The inside of the housing case was redesigned to remove and reshape ribs to decrease resistance and increase the visibility during assembly. The bracket used to attach the motor was redesigned to allow unobstructed access to the motor mount. It should be noted that these design changed did not eliminate any of the parts, but only eliminated the difficulties in assembling the current parts, and thus did not change the connectivity graph. The assembly time for this design by Boothroyd and Dewhurst assembly time estimation is 201 s.

5. Validation set

Validation of the model requires a second set of systems which are not used in model development. A set of three systems is used, consisting of a clicker pen, an electric can opener and a cordless drill. This set is drawn from the same undergraduate/graduate design for manufacturing and assembly course as the majority of the training set. However, these systems are addressed only in their original form without an accompanying redesigned version. Like the training set, the assembly time analysis for each of these systems is performed by different individuals and taken to be correct.

5.1. Clicker pen

The clicker pen, shown in Figure 12, is a very small system consisting of only eight total parts. Most notably, there are virtually no fasteners, with the exception of the single spring powering the clicker system. All remaining parts use integrated fastening elements or simple surface contact in their connections. A curious feature in regards to the connectivity graph of this system is the fact that the ink cartridge only interacts with the housing through the spring connection. Boothroyd and Dewhurst assembly time analysis estimates the assembly time of this system to be 34.66 s.

5.2. Electric can opener

The electric can opener uses a magnet to suspend the can from a removable cuttings assembly and drives the can with an exposed spur gear. This is seen in Figure 13. The housing encloses a flat form factor brushless motor, gear train and an electric switch assembly. The motor in this system is unique in that the rotor and stator are separate pieces which must be positioned in the assembly process. This is unusual in the connectivity of the system in that the rotor and stator are not physically connected in a brushless motor. The assembly time for this system by Boothroyd and Dewhurst assembly time estimation is 292.22 s.

Figure 12. Clicker pen. Note: http://www.officespecialties.com/pilot_31277_g2_ultra_fine_retractable_pen_42038_prd1.htm, accessed on 25 February 2011.

Figure 13. Electric can opener.

5.3. *Cordless drill*

The cordless drill, shown in Figure 14, is notable for a high degree of interconnection. Nearly all primary parts in this system interact with both halves of the housing. Also of interest in this system is the presence of wire connectors which must be pressed together with some force, in addition to several screw fasteners with longer than normal engagement lengths. The assembly time for this system by Boothroyd and Dewhurst assembly time estimation is 128.06 s.

6. Model development

To develop a model for prediction of assembly time, a pattern must be identified between complexity metric results and DFA results. Rigorous model development protocols require numerous data points which are not available at this time. As such, a more rudimentary pattern recognition approach is applied to demonstrate the capability of complexity metrics to form a surrogate mapping between physical system architecture and approximate assembly time. It should be noted that the specific model developed here is generalisable only to systems similar to those included in the training set and is not intended as a model for all assembly operations.

6.1. *Training set complexity metric results*

First, the training set of products and their redesigned forms must be evaluated on the complexity metrics described in Section 3. These are presented in Table 1 through Table 3. Table 1 provides the results for the size metrics discussed in Section 3.1. Likewise, Table 2 provides results for the path length metrics presented in Section 3.2 and Table 3 provides results for the decomposition metric presented in Section 3.3.

Figure 14. Cordless drill.

6.2. *Metric–assembly relationship*

The next step in this process is to visualise the relationship between the various metrics and the Boothroyd and Dewhurst assembly time estimation analysis results. This is done by plotting the DFA results for each system against each metric. Figure 15 shows this for size metrics for all systems other than the Tweel™ variations. This is due to the significantly higher order of the Tweel™ metrics and DFA results. From this plot, it can be observed that the general

Table 1. Size metrics for training set.

	Elements	Rel.	Conn.	DOF
Shifter original	22	23	62	55
Shifter redesign	13	19	46	35
Mixer original	24	23	59	52
Mixer redesign	15	17	40	29
Chopper original	36	37	93	81
Chopper redesign	36	35	79	79
Knife original	49	64	160	132
Knife redesign	38	51	126	105
Tweel™ original	1190	524	2023	3029
Tweel™ redesign	613	531	1971	2802

Table 2. Path length metrics for training set.

	Total	Max	Average	Density
Shifter original	948	3	2.05	0.0892
Shifter redesign	272	2	1.74	0.0918
Mixer original	1118	4	2.22	0.1010
Mixer redesign	490	5	2.33	0.1373
Chopper original	3226	5	2.56	0.0692
Chopper redesign	3226	5	2.56	0.0732
Knife original	6110	4	2.60	0.0406
Knife redesign	3450	4	2.45	0.0481
Tweel™ original	3,544,532	6	2.51	0.0048
Tweel™ redesign	892,240	7	2.38	0.0045

Table 3. Decomposability metric for training set.

	Ameri–Summers
Shifter original	36
Shifter redesign	44
Mixer original	21
Mixer redesign	29
Chopper original	74
Chopper redesign	61
Knife original	273
Knife redesign	218
Tweel™ original	641
Tweel™ redesign	1869

trend is for assembly time to increase dramatically with increasing size. The plots for path length and decomposition metrics are not shown here for space purposes. It should be noted, however, that among those metrics only total and average path length produced consistent trends.

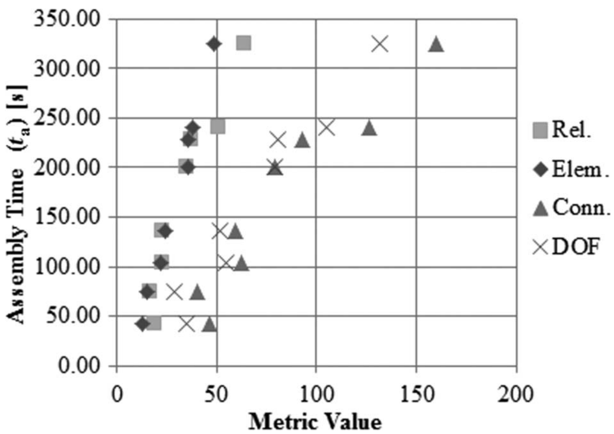

Figure 15. Size metric plot.

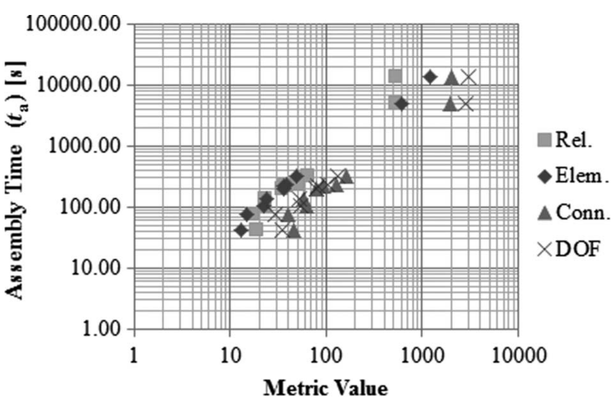

Figure 16. Log–log size metric plot.

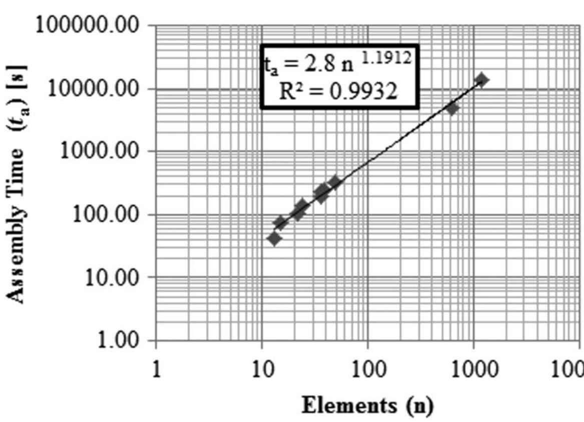

Figure 17. Power regression of part count – assembly time trend.

To better visualise the size trends, seen in Figure 15, such that the Tweel^{TM} results may be considered, a log–log plot of the same data was created. This is shown in Figure 16. Here, it can be seen how the size metrics for the consumer products line up with those from the Tweel^{TM}. The assembly time values for most of these measurements still reflect a dramatically higher slope for the Tweel^{TM} than the other systems, despite the log–log format. However, there is one notable exception. Elements, representing the count of primary and fastening parts, appear as a nearly straight line for all systems including both variations of the Tweel^{TM}. Such a consistent trend with regards to part count is not entirely surprising as the positioning of each individual physical element is a significant driving force in assembly time.

6.3. *Regression*

The next step is to establish a rough model through regression. A series of regression models are generated for each of the metrics using linear, polynomial, power, exponential and logarithmic models. These regression models are each evaluated for their correlation with the sample data. As the relationship between part count and assembly time appears linear in a log–log plot, it follows that the appropriate model for this trend is that

Table 4. Error in regression model.

	DFA time (s)	Reg. time (s)	% Error
Shifter original	104.56	146.70	40%
Shifter redesign	42.60	75.29	77%
Mixer original	104.56	170.25	25%
Mixer redesign	42.60	102.33	37%
Chopper original	136	256.53	12%
Chopper redesign	74.7	260.23	29%
Knife original	228.5	338.49	4%
Knife redesign	201	254.34	6%
Tweel^{TM} original	13,561.35	13,362.01	−1%
Tweel^{TM} redesign	4925.00	6032.32	22%

Table 5. Error in refined model.

	DFA time (s)	Model time (s)	% Error
Shifter original	104.56	105.37	1%
Shifter redesign	42.60	46.10	8%
Mixer original	136	132.28	−3%
Mixer redesign	74.7	83.76	12%
Chopper original	228.5	229.20	0%
Chopper redesign	201	232.50	16%
Knife original	325.00	306.26	−6%
Knife redesign	240.00	217.71	−9%
Tweel^{TM} original	13,561.35	11,430.28	−16%
Tweel^{TM} redesign	4925.00	4919.21	0%

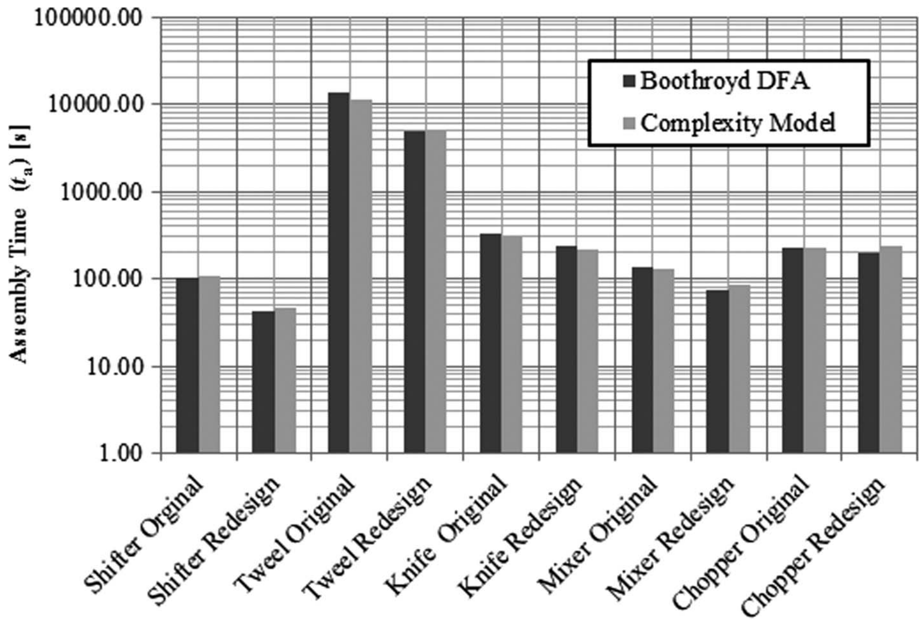

Figure 18. Refined model results.

Table 6. Complexity metrics for validation set.

	n	APL	PLD
Clicker pen	8	1.93	0.2411
Electric can opener	40	2.82	0.0672
Cordless drill	25	1.94	0.0440

Table 7. Validation set results.

	DFA time (s)	Model time (s)	% Error
Clicker pen	34.66	37.42	8%
Electric can opener	292.22	286.15	−2%
Cordless drill	128.06	101.19	−21%

of a power regression. This is confirmed by the fact that this combination of metric and regression model yielded the highest correlation of any combination. The regression is computed automatically by software and results in the line and equation shown in Figure 17. The high R-squared value quoted here is the result of the very large range over which the model is applied with limited intermediate values.

6.4. *Refinement*

The accuracy of the regression, while exhibiting strong correlation, is far from perfect. To better understand the accuracy of this model, Table 4 shows how the percent error in the regression model varies between −1% and +77%. This shows significant over estimation in the regression model, particularly with very small systems.

To correct for this large discrepancy, it is suggested that additional metrics may be used to supplement the model by replacing in whole or in part the constants derived by the regression. To this end, it is observed that the coefficient of the regression, 2.80, is very similar to the average path length of the systems, which range between 1.74 and 2.51. The value of average path length was also observed to be roughly proportional to estimated assembly time. Thus, the constant coefficient of the equation is replaced with average path length to introduce the proportional trend.

This brings values closer to the DFA estimates with the exception of the values are now underestimated with an error range of −28% to +1%. To correct for this, it is suggested that the exponent of the regression, 1.1912, be supplemented through the use of path length density. The value for path length density is never greater than one, is typically on the order of hundredths or less, and decreases with increasing system size. Thus, it is proposed that the path length density be added to provide a slight increase to and a finely granular step down of the exponent as the system size increases.

The final step in refinement is to tune the resulting model to the available DFA estimates to minimise the average absolute percent error. This is done by adjusting the constant in the exponent to the third decimal place. Tuning to higher significant digits does not produce appreciable change in results. These alterations to the model result in Equation (1) where t_a is assembly time, APL is average path length, n is the

Table 8. Sensitivity of Boothroyd and Dewhurst assembly time estimation.

	St. Dev.			Maximum		Minimum	
	Mean (s)	Δ (s)	%E	Val (s)	%E	Val (s)	%E
Clicker pen	42.5	8.07	19%	57.15	34%	23.3	45%
Gear shifter	141.82	37.12	26%	204.94	45%	104.19	27%
CD changer	54.3	11.4	21%	74.68	38%	45.92	15%
Fuel tank	126.98	25.29	20%	171.99	35%	106.97	16%
	Mean %E:		22%	Mean %E:	38%	Mean %E:	26%

number of elements and PLD is path length density. As this model is a surrogate mapping as opposed to a physical relationship, all of the parameters within the model are taken to be unitless with a unit second applied to the result.

$$t_a = [\mathrm{APL}] \times n^{(1.185+[\mathrm{PLD}])} \quad (1)$$

When this refined model is applied to the training set, the results are those shown in Table 5 and illustrated in Figure 18. The percent error is reduced to $\pm 16\%$. Additionally, it can be seen that the ordinal change between the original and redesigned version of each system is correctly predicted for all but the chopper. This discrepancy is due to the fact that the redesign of the chopper primarily addressed geometric changes for ease of access in assembly operations and included the removal of some assembly feature symmetry for manufacturing savings. As this model is driven by system architecture and not geometry, it is to be expected that only the increase in assembly due to the loss of feature symmetry would be captured.

6.5. *Validation*

To ensure that the developed model remains valid when applied outside of the training set, the results of the developed model are compared in regards to the results of Boothroyd and Dewhurst assembly time estimation for the previously established validation set. These are subjected to the same complexity metrics as the training set. The metrics pertinent to the proposed model are summarised in Table 6. This again demonstrates the independence of the individual metrics.

Applying the complexity metric values to Equation (1) yields the values shown in Table 7. The percent errors in the cases of the clicker pen and electric can opener are within the same range seen for the training set. The percent error on the cordless drill falls well outside of this range at -21%. However, this result does not invalidate the model.

The data in Table 8, derived from work on the sensitivity of Boothroyd and Dewhurst assembly time estimation to subjective information by (Namouz *et al.* 2012), suggest the acceptable limits on any model derived from this estimation. The standard deviation in the assembly time estimation for these products when all possible subjective answers are considered is equivalent to a 22% error on average. Further, the typical maximum and minimum observed values are equivalent to 38% and 26% error, respectively. Thus, all of the validation set results fall within one standard deviation and well within the possible maximum and minimum objective values for Boothroyd and Dewhurst assembly time estimation. In fact, the first product in Table 8 represents the same clicker pen system addressed here and shows how the estimate used in validation differs from the mean value observed by Namouz *et al.* (2012).

7. Conclusions and future work

The example model developed here has shown an ability to predict the assembly time of a system based on the physical architecture of that system. The variability of the model with respect to the results of a traditional Boothroyd and Dewhurst assembly time estimation analysis are within one standard deviation of that possible between different designers conducting the same assembly time analysis. This is highlighted even more by the fact that the analysis on all of the systems in both the training and validation set were in fact conducted by different designers. Thus, the model has been observed to be preliminarily valid for extension to new systems within the tested range of consumer products.

This demonstrates the ability of complexity metrics to be used to predict properties of the final design. While the method applied to the development of the model shown here lacks the rigor of a more formalised model development method, the level of correlation and accuracy which can be achieved through these means is equivalent to that of existing, manual effort intensive methods which require greater input information and, thus, a more developed design. This is suggestive of the power of mapping complexity values to measures of interest.

Further research should apply additional systems to the model without further tuning, as well as extension of the method to other classes and physical scales of assembled systems. This will further validate the approach as a tool which may be used in practice and may reveal the underlying mechanisms of structural complexity which drive assembly time. Of particular interest is the behaviour of the tuned exponent value for training sets of different classes and physical scales. It is hypothesised that this value may function as a scaling factor. Furthermore, for any complexity-based model to be applicable with confidence, a much larger study would need to be performed based upon observed assembly times in practice. This is a practical goal for the development of a model in an industrial setting where significant process data are available and the set of systems considered is highly specific.

An additional point of interest is the extension of complexity modelling methods to other measures of interest. These may include any number of designs for X analysis, design performance and product performance measures. For example, the model here is independent of geometry but it may be possible to produce a model, based on CAD representations, which is an analog for design for manufacturing analysis or as a complete prediction of system production cost.

Acknowledgements

The authors would like to recognise the efforts of the students and members of our research group which helped provide us with source data and those figures for which a specific source was not cited.

References

Ameri, F., *et al.*, 2008. Engineering design complexity: an investigation of methods and measures. *Research in Engineering Design*, 19 (2–3), 161–179.

Boothroyd, G., 1994. Product design for manufacture and assembly. *Computer-Aided Design*, 26 (7), 505–510.

Boothroyd, G., 2005. *Assembly automation and product design*. 2nd ed. Boca Raton, FL: Taylor & Francis.

Boothroyd, G. and Alting, L., 1992. Design for assembly and disassembly. *CIRP Annuls 1992 Manufacturing Tecnology*, 41 (2), 625–636.

Boothroyd, G. and Dewhurst, P., 1980. *Product design for assembly*. Wakefield, RI: Boothroyd and Dewhurst, Inc.

Boothroyd, G. and Dewhurst, P., 1988. Product design for manufacture and assembly. *Manufacturing Engineering*, 100 (4), 42–46.

Boothroyd, G. and Walker, J., 1996. Design for assembly. *In*: J.Walker, ed. *Handbook of manufacturing engineering*. New York: Marcel Dekker.

Dalgleish, G.F., *et al.*, 2000. Design for assembly: influencing the design process. *Journal of Engineering Design*, 11 (1), 17–29.

Leaney, P.G., 1996. Case experience with design for assembly methods. *In*: G.Q. Huang, ed. *Design for X: concurrent engineering imperatives*. London, UK: Chapman & Hall.

Mascle, C., 2003. Decision support system in a design for assembly and disassembly methodology. *In*: A. Bourjault and A. Delchambre, eds. *Proceedings of the 5th IEEE international symposium on assembly and task planning*, 10–11 July, Besancon, France, 216–221.

Mathieson, J.L., Sen, C., and Summers, J.D., 2009. Information generation in the design process. *In*: K. Anderson, *et al.*, ed. *Proceedings of the ASME 2009 international design engineering technical conferences & computers and information in engineering conference*, 30 August–2 September, San Diego, CA, USA.

Mathieson, J. and Summers, J., 2009. Relational DSMs in connectivity compexity measurement. *In*: G. Fadel *et al.*, eds. *11th international DSM conference*, 12–13 October, Greenville, SC.

Mathieson, J.L. and Summers, J.D., 2010. Complexity metrics for directional node-link system representations: theory and applications. *In*: P. Larochelle and A. Murray, eds. *Proceedings of the ASME IDETC/CIE 2010*, 15–18 August, Montreal, Quebec, Canada.

Mital, A., *et al.*, 2008. *Product development: a structured approach to consumer product development, design, and manufacture*. Oxford, UK: Butterworth-Heinemann.

Namouz, E.Z., *et al.*, 2012. Reasoning: source of variability in the Boothroyd and Dewhurst assembly time estimation method. *In*: M. Stanisic, *et al.*, eds. *Proceedings of the ASME 2012 IDETC/CIE*, ASME, 12–15 August, Chicago, IL, USA.

Ohashi, T., *et al.*, 2002. Extended assemblability evaluation method (AEM). *JSME International Journal*, 45 (2), 567–574.

Priest, J. and Sanchez, J., 2001. *Product development and design for manufacturing*. New York: Marcel Dekker.

Summers, J.D. and Shah, J.J., 2010. Mechanical engineering design complexity metrics: size, coupling, and solvability. *Journal of Mechanical Design*, 132 (2), 021004 (11 Pages).

Warnecke, H.J. and Babler, R., 1988. Design for assembly – part of the design process. *CIRP Annuls 1988 Manufacturing Technology*, 37 (1), 1–4.

Welter, T., 1989. Designing for manufacture and assembly. *Industry Week*, 238, 79–82.

Yamigiwa, Y., Negishi, T., and Takeda, K., 1999. Life cycle design achieving a balance between economic considerations and enviromental impact with assembly-disassembly evaluation/design DAC (design for assembly/disassembly cost-effectiveness). *In*: *Proceedings of the first international symposium on environmentally conscious design and inverse manufacturing*, 1–3 February, Tokyo, Japan, 760–765.